Wear 444-445 (2020) 203159

Contents lists available at ScienceDirect

Wear

journal homepage: http://www.elsevier.com/locate/wear

# The effect of nanoclay particles on the incubation period in solid particle erosion of glass fibre/epoxy nanocomposites

Mehmet Bagci [a,*], Musa Demirci [b], Emine Feyza Sukur [a], Halil Burak Kaybal [c]

[a] Konya Technical University, Engineering and Natural Science Faculty, Mechanical Engineering Department, Konya, Turkey
[b] KTO Karatay University, Engineering Faculty, Mechanical Engineering Department, Konya, Turkey
[c] Amasya University, Technology Faculty, Department of Mechanical Engineering, Amasya, Turkey

ARTICLE INFO

*Keywords:*
Solid particle erosion
Polymer matrix composite
Nanotribology
Erosion testing
Surface analysis

ABSTRACT

During erosion tests of glass fibre/epoxy nanocomposites, an incubation period emerged because of the embedding of abrasive particles into the target material. In this study, the effect of this period on solid particle erosion behaviour was investigated for glass fibre/epoxy composites with the addition of nanoclay. The surface erosion characteristics of the composites were obtained by solid particle erosion tests using angular alumina particles with a size on the order of 400 μm as the erodent. The tests were conducted using impact velocities of ~23 or ~34 m/s and impingement angles of 30°, 60° or 90° as operating conditions. The eroded surfaces were examined using a scanning electron microscope to characterise the incubation mechanisms taking place in the nanocomposites. The glass fibre/epoxy composite without nanoclay (the pure test specimen) had the highest erosion resistance when compared to the composites with a nanoclay additive in ratios between 1% and 3% by weight. The findings of this study indicate that the agglomeration and weak compatibility of nanoclay, glass fibre and epoxy affected the results.

## 1. Introduction

Polymers and their composites are widely used as structural materials for different machine components and engineering systems because of their specific properties. Some examples of the application of polymer composites include sand-transporting pipelines, sludge transportation lines in oil refineries, rotor blades for helicopters, pump propulsion fins, high-speed vehicles and planes, plane motor fins and missile components. An important property in these types of applications is resistance to particle erosion because these parts are often used in environments with abrasive particles [1].

One of the methods for improving the properties of polymers and their composites (mechanical, tribological, etc.) is the addition of some kind of reinforcement into the matrix. The types of reinforcements used to improve the erosion wear performance of composite materials tend to be classified in the literature as whiskers, layered materials, fibres (glass, carbon, Kevlar, basalt, etc.) and particles–microparticles ($Al_2O_3$, $SiO_2$, $B_2O_3$, SiC, WC and TiC) [2–6] or nanoparticles (NC, CNT and ceria) [7–9]. In recent years, there has been growing interest in the use of nanoparticles and inorganic fillers in polymer matrix composites to improve their properties. Owing to the large surface area of these nanoparticles (1000 $m^2/g$) [10], the load is transferred from the matrix to the nanoparticles, and the mechanical properties of the matrix can be improved [11]. When considering their load-bearing capacities, carbon nanofibres, nanotubes and nanoclays (NC) are optimal candidates for such fillers.

Nanofilled polymers, defined as polymeric nanocomposites (PNCs), contain a homogeneously dispersed phase with nanometric dimensions in a continuous polymer matrix and behave like a single-component, single-phase material. These PNCs usually contain from 1% to 3% nanoparticles by weight. Nanoreinforcements have enhanced properties such as low density, non-flammability, good thermal conductivity and presenting as a gas barrier. The two fundamental factors affecting these properties are the good distribution of the nanoparticles in the resin-reinforcement system and strong interfacial interactions between the nanoparticle layer and the matrix [12]. Other factors affecting the final properties of nanocomposites are the type and size of filler material, its volume percentage, the compatibility between the nanofiller and the polymer matrix, the process parameters and the curing conditions [13].

Clay is the most commonly used and most widely examined nanofiller among those that are applied to polymer nanocomposites doped with nanoparticles. Because of its availability and nature, it is

* Corresponding author.
*E-mail addresses:* mbagci@ktun.edu.tr, meh_bagci@yahoo.com (M. Bagci).

https://doi.org/10.1016/j.wear.2019.203159
Received 20 March 2019; Received in revised form 5 December 2019; Accepted 12 December 2019
Available online 13 December 2019

increasingly used in enhancing the mechanical and tribological properties of composite materials [14]. One of the most commonly used types of clay is montmorillonite clay, the dominant components of which are silica and alumina. Montmorillonite has a high elastic modulus, low material cost, low density, high thermal stability, low thermal expansion coefficient and sufficiently high specific surface area [15]. All of these properties significantly enhance the strength, hardness, fracture toughness, dimensional stability and thermo-mechanical behaviour of nanoparticle-reinforced polymers [16]. The literature reveals that a considerable number of studies have been conducted on the effects of nanoclay on the mechanical and tribological properties of nanocomposites [17–19].

In this experimental study, nanoclay was added to glass fibre/epoxy (GF/epoxy) composites, and the erosion wear behaviours of these composites were examined under three different impingement angles (30°, 60° and 90°), two impact velocities (~23 or ~34 m/s) and two abrasive masses (5 and 10 kg). Nanoclay was added in a ratio of 1% and 3% by weight to the glass fibre/epoxy composite, and the weight losses and erosion rates of these specimens were compared to each other. In addition, scanning electron microscope (SEM) images of specimens' surfaces were examined, and the effects of nanoreinforcement on the results were interpreted.

## 2. Materials and methods

### 2.1. Materials and specimen preparation

Laminating epoxy resin MGS-L285 with a low-viscosity, two-phase structure (80%–90% diglycidyl ether bisphenol A and 10%–20% aliphabit diglycidyl ether mixture) and curing agent MGS-H285 (70%–80% cycloaliphatic amine and 10%–30% polyoxyl alkyl amine mixture) were chosen for this study. The epoxy resin was supplied by Momentive Hexion Inc. The nanoclay was purchased from Esan Chemical Industry. Owing to the layered structure of montmorillonite clays, its surface properties can be modified. Although the initial inter-layer distance of the nanoclay is approximately 15 Å, this value can be in the range of approximately 38–40 Å with organic modification. This increase in the spacing between the layers ensures the homogeneous distribution of the clay in the polymer structure. The details of the chemical composition of the nanoclay are given in Table 1.

Fibre reinforced composite materials consist of at least two main phases. These are the reinforcement (glass, carbon, basalt, etc.) phase and the matrix (polyester, epoxy, vinylester, etc.) phase. The reinforcement phase has already good strength itself. The phase which weakens the composite material is the matrix phase. Therefore, the selection or modification of the matrix phase directly affects the mechanical properties of the composite material.

The nanocomposite materials used in the erosion tests were produced with 1% and 3% nanoclay doping ratios. The desired weight ratio of nanoclay addition was incorporated into the epoxy polymer. The nanoclay was first mixed into the epoxy using a mechanical mixer (Qsonica WF-OD20). This process continued for 1 h until the nanoclay was fully wetted by the epoxy. The mixture was then mixed using an ultrasonic mixer to ensure homogeneous dispersion of the nanoclay. This mixing process was carried out using an ice bath to minimise the temperature rise that occurs during mixing. The ultrasonic mixing process was also performed for 1 h. Finally, a curing agent was added to the nanoclay/epoxy system, which was distributed homogeneously according to the supplier's instructions. After this final stage, the nanocomposite matrix material was ready. A detailed flow diagram of the production of the nanoclay/epoxy matrix is shown in Fig. 1.

The schematic stages of the manufacture of the composite materials are shown in Fig. 2. The nanoclay/epoxy matrix was first impregnated using the hand lay-up technique with glass fibres. After all of the fibres were impregnated, the excess polymer on the fibres was ejected by the vacuum infusion method. At the last stage, the curing process was performed for 1 h at 100 °C and 2 h at 120 °C to prevent any residual stress that would arise from irregularities within the material.

The glass fibres used in the experiments have a 0°/90° woven-type weave structure and a weight of 200 g/m$^2$. Composite plates were obtained by combining the cured glass fibre/epoxy sheets. Composite plates of 2.4 ± 0.1 mm in thickness and 350 × 500 mm in size were then cut using a diamond saw to reduce their size to 30 × 30 mm, which is appropriate for erosive wear tests. Table 2 shows the mechanical properties of all test specimens for comparison. The porosity of the materials was not measured. However, it was obtained from the material manufacturer that 2–3% porosity is mostly due to production.

### 2.2. Solid particle erosion test

Tests were performed in a specifically designed erosive wear test rig in compliance with ASTM G76-95 standard test method. The testing environment is dry and pressurised air, in which abrasive particles were set to impact the test specimen surface. The schematic representation of the test rig is shown in Fig. 3(a). The abrasive particles and air are mixed in the mixing chamber by being pressurised. The abrasive particle reservoir is filled with the abrasive particles whose weight is known before. The flow rate of abrasive particles is adjusted with Pressure Regulator 2 in the test rig.

The geometry of the specimens used in this test method is simple and small-scaled, which enables easy examination of dimensional changes and weight loss in wear measurements. The impingement angle is one of the most important parameters affecting erosion, and it can be changed by the adjustment apparatus detailed in Fig. 3(b). In the erosion wear tests, the impingement angles of 30°, 60° and 90° can be easily adjusted in 15° sensitivity intervals using this apparatus. In addition, the distance between the nozzle and the test specimen can be simply set by moving the specimen holder up or down. Alumina ($Al_2O_3$) particles have commonly been used in the literature as abrasive particles. Alumina has a high abrasion resistance because of its ceramic properties and high thermal resistance.

High-speed photography [20], laser doppler anemometers [21] and the double-disc method [22] are considered standard measurement techniques when determining the impact velocity of erosion particles, which is an important factor in erosion wear. Among these, the double-disc method is the most widely used since it is more economical and simpler to install. Thus, this method was used for the measurement of impact velocities in this study. The details of the test parameters are given in Table 3.

To determine the weight loss; weight of each test specimen was measured before and after tests. After determining weight loss of the specimen, erosion rate (E) is calculated according formula given below:

$$E = \frac{\text{weight loss of the specimen (mg)}}{\text{mass of erosive particles striking the surface (kg)}} \quad (1)$$

**Table 1**
Chemical composition of nanoclay.

| Materials | % $Al_2O_3$ | % $SiO_2$ | % $Na_2O$ | % $Fe_2O_3$ | % $K_2O$ | % CaO | % MgO | % $TiO_2$ | % LOl |
|---|---|---|---|---|---|---|---|---|---|
| Percent (%) | 6,0 ± 1,0 | 44 ± 1,0 | 0,6 ± 0,2 | 0,4 ± 0,2 | 0,3 ± 0,1 | 0,4 ± 0,1 | 1,4 ± 0,2 | 0,05 ± 0,02 | 45 ± 2,0 |

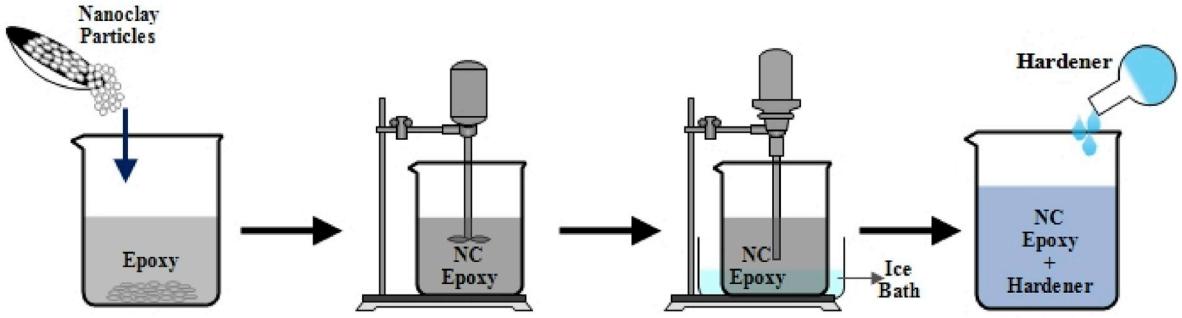


**Fig. 1.** Production of nanoclay doped epoxy matrix.

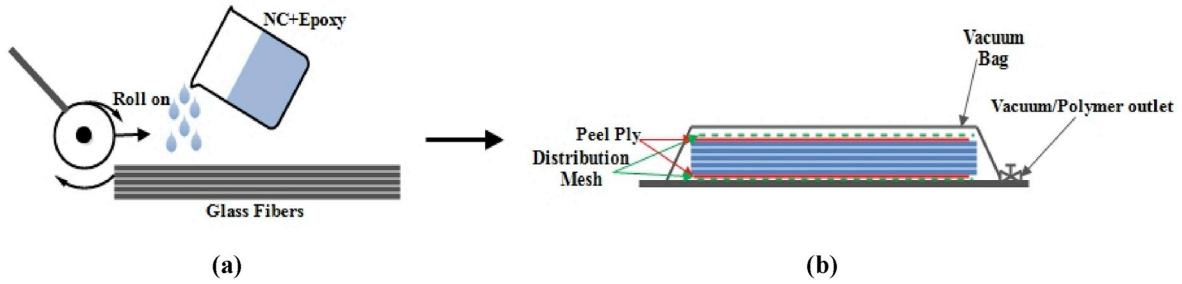


**Fig. 2.** Manufacturing of composite materials; a) Hand-lay-up technique, b) Vacuum infusion method.

**Table 2**
Mechanical properties of the test specimens.

| Property | GF/epoxy (pure) | 1% NC/ epoxy | 3% NC/ epoxy |
|---|---|---|---|
| Fiber diameter (μm) | 14 | 14 | 14 |
| Fiber aerial weight (g/m$^2$) | 300 | 300 | 300 |
| Fiber density (g/cm$^3$) | 2.6 | 2.6 | 2.6 |
| Density (g/cm$^3$) | 1.724 | 1.743 | 1.768 |
| Hardness (shore D) | 89.7 | 88 | 86.8 |
| Fiber/volume ratio (±3%) | 50 | 50 | 50 |
| Resin/volume ratio (±3%) | 50 | 49 | 47 |
| Nanoclay percentage by weight (±0.01) | 0 | 1 | 3 |

## 3. Result and discussions

### 3.1. The effect of impingement angle, impact velocity and abrasive mass

The specimens of glass fibre/epoxy composite [GF/epoxy (pure), 1% NC/epoxy, 3% NC/epoxy] were exposed to erosion wear with two different impact velocities (~23 or ~34 m/s), three different impingement angles (30°, 60° and 90°), and ~400 μm sized abrasive particles. The weight losses based on impingement angles were given by graphs below. In order to determine points on the graph, three tests were conducted for each situation and graph was drawn by using the obtained average value from those three tests. This is important to obtain reliable results. Fig. 4 shows the weight loss changing of the test specimens according to abrasive mass, impingement angle, and abrasive particle

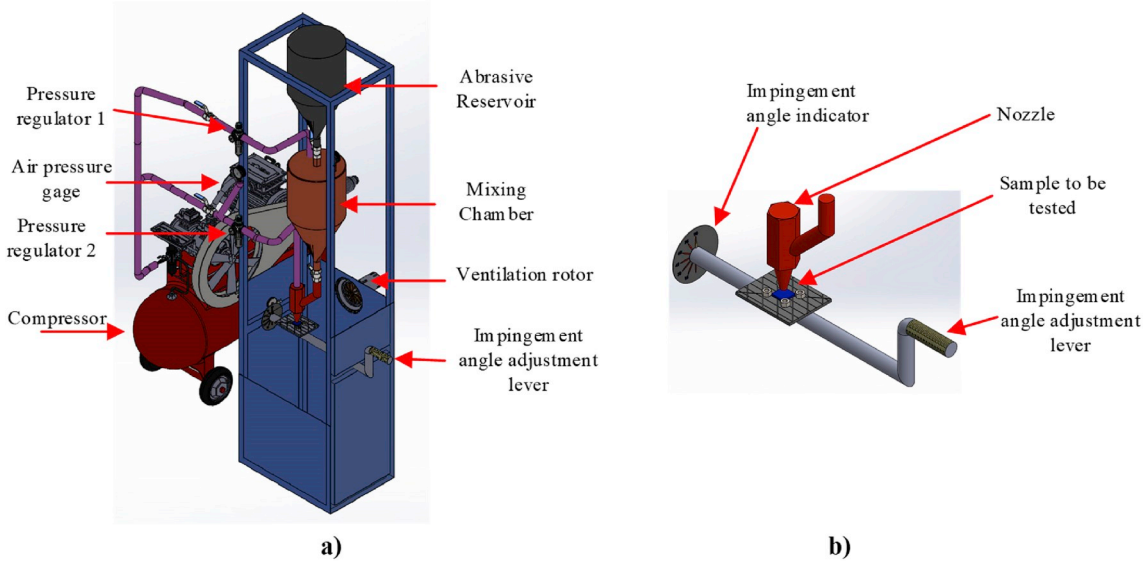


**Fig. 3.** Solid particle erosion test rig; a) 3D drawing, b) Impingement angle adjustment lever.

**Table 3**
Erosion test conditions.

| Test Parameters | GF/epoxy (pure, 1% and, 3% NC) |
|---|---|
| Erodent | Alumina ($Al_2O_3$) |
| Erodent size (μm) | ≈400 |
| Erodent shape | Angular |
| Erodent flow rate (g/s) | 165, 185 |
| Impingement angle, α (°) | 30, 60, 90 |
| Test temperature (°C) | Room temperature |
| Abrasive mass (kg) | 5, 10 and 20 |
| Test duration (min) | ~20 |
| Nozzle to specimen distance (mm) | 10 |
| Nozzle diameter (mm) | 6 |
| Nozzle length (mm) | 86 |
| Impact velocity (m/s) | ~23, 34 |

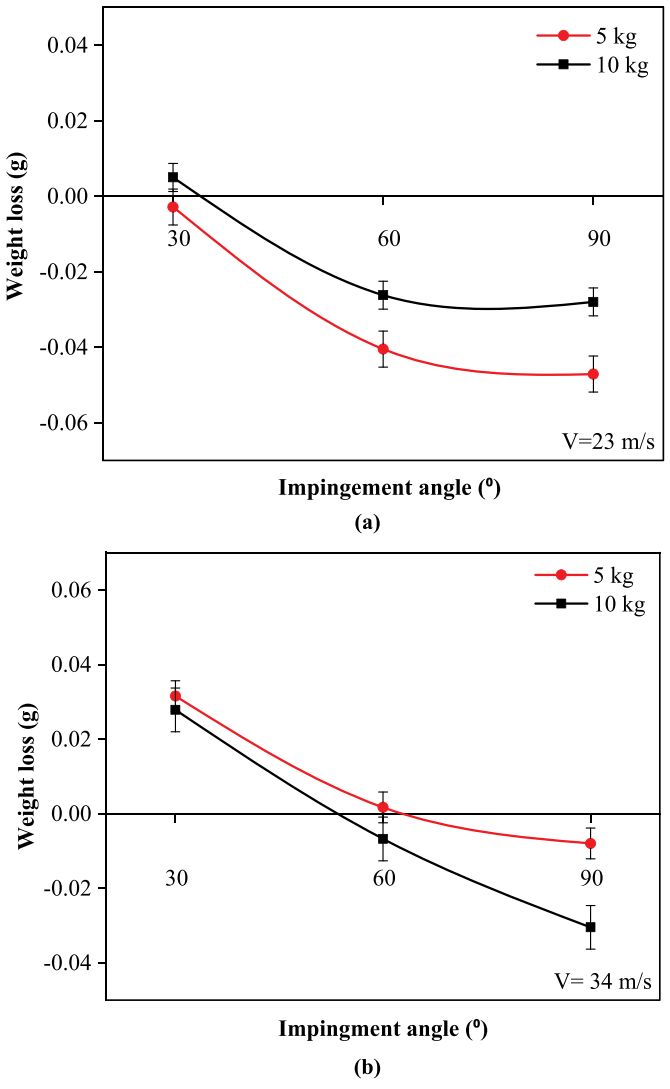


**Fig. 4.** The impingement angle-weight loss relation of the GF/epoxy (pure) test specimens under different abrasive masses (5, 10 kg): a) 23 m/s, b) 34 m/s.

impact velocity.

As known from the literature, when mass loss is measured as a function of impingement angle, ductile materials show maximum erosion rate with low impingement angles (15°–30°). As it can be seen from Fig. 4, GF/epoxy (pure) test specimens show a similar tendency when compared to ductile materials in the literature [2,3].

In the weight loss vs impingement angle and time graphs, the positive zone represents mass loss, and the negative zone represents mass gain. Upon examination of the 23 m/s impact velocity, shown in Fig. 4 (a), it can be seen that the specimen gained weight when the test was conducted with a 30° impingement angle and 5 kg total mass of abrasive particles.

Owing to the ductile properties of the material, solid particles were embedded into the surface during abrasive particle impact, and this situation can be described as the incubation period for the impingement angle. After doubling the abrasive particle mass, the particles continued to embed into the surface. However, at a further stage, the matrix started to break, and the specimen weight decreased because of a ploughing effect on the surface. By increasing the impingement angle from 60° to 90°, the effect of embedding on the surface became more evident, and the weight increased further. When the impingement angle is normal to the nozzle, the abrasive particles accumulating on the specimen positively contribute to its mass. The incubation period took place at an impact velocity of 34 m/s and an impingement angle of 30°. In addition to this, the abrasive particles were beginning to separate from the material surface [Fig. 4(b)]. However, when the abrasive mass was increased from 5 to 10 kg, the weight loss decreased at a 30° impingement angle. In the tests conducted with 10 kg abrasive mass, it was observed that more abrasive particles were embedded, and the process of separation from the surface took longer. The fact remains that the erosion rate increased using 5 kg total mass of abrasive particles. This can be attributed to the short incubation period from the transition process to steady-state erosion wear.

An increase in specimen weight was observed depending on the embedding value when the abrasive mass was increased from 5 to 10 kg at 34 m/s impact velocity and impingement angles of 60° and 90°. The trends are similar for impingement angles of 60° and 90°, However, in the case of 60°, the embedded abrasive particle mass decreased, but the incubation period had continued. The findings of this study agreed with previous works, which state that the incubation period decreases with an increase in impact velocity and a decrease in impingement angle [23, 24].

Beside the weight loss, volumetric loss in the test specimen were also measured. The comparison of volumetric wear rate in test specimens is given in Table 4. Volumetric loss were calculated by 3D scanner (Nanomap - 500LS, AEP, CA, USA) and the trends in the mass and volumetric loss were similar.

The eroded surface morphologies of the composite specimens were examined using a SEM. The SEM images of the eroded surface of the glass fibre/epoxy composite specimens at 34 m/s impact velocity for three different impingement angles (30°, 60° and 90°) are shown in Fig. 5. From SEM observations, it appears that the material is mostly removed from the target surface by microcutting and microploughing. At impingement angles of 60° and 90°, the abrasive particles embedded in the test specimens were seen, as shown in Fig. 5(b) and (c), and it was observed that they might influence the incubation period. The main damage mechanisms of solid particle erosion on the test specimens are characterised by fibre matrix debonding, fibre breakage, matrix cracking, material removal and crater formation [Fig. 5(a), (b) and (c)].

Impact velocity is an important parameter in solid particle erosion. A higher impact velocity results in increased deformation on the specimen surface. When the SEM images in Fig. 6 are examined, it can be seen that deeper and larger craters are formed as a result of the higher impact

**Table 4**
Comparisons of volumetric losses in test specimens.

| Test Specimen | Impingement Angle (°) | Impact Velocity (m/s) | Volumetric Wear Rate ($mm^3sec^{-1}$) |
|---|---|---|---|
| GF/epoxy (pure) | 30 | 34 | 0,14 |
| 1% NC/ epoxy | 30 | 34 | 0,29 |
| 3% NC/ epoxy | 30 | 34 | 0,25 |

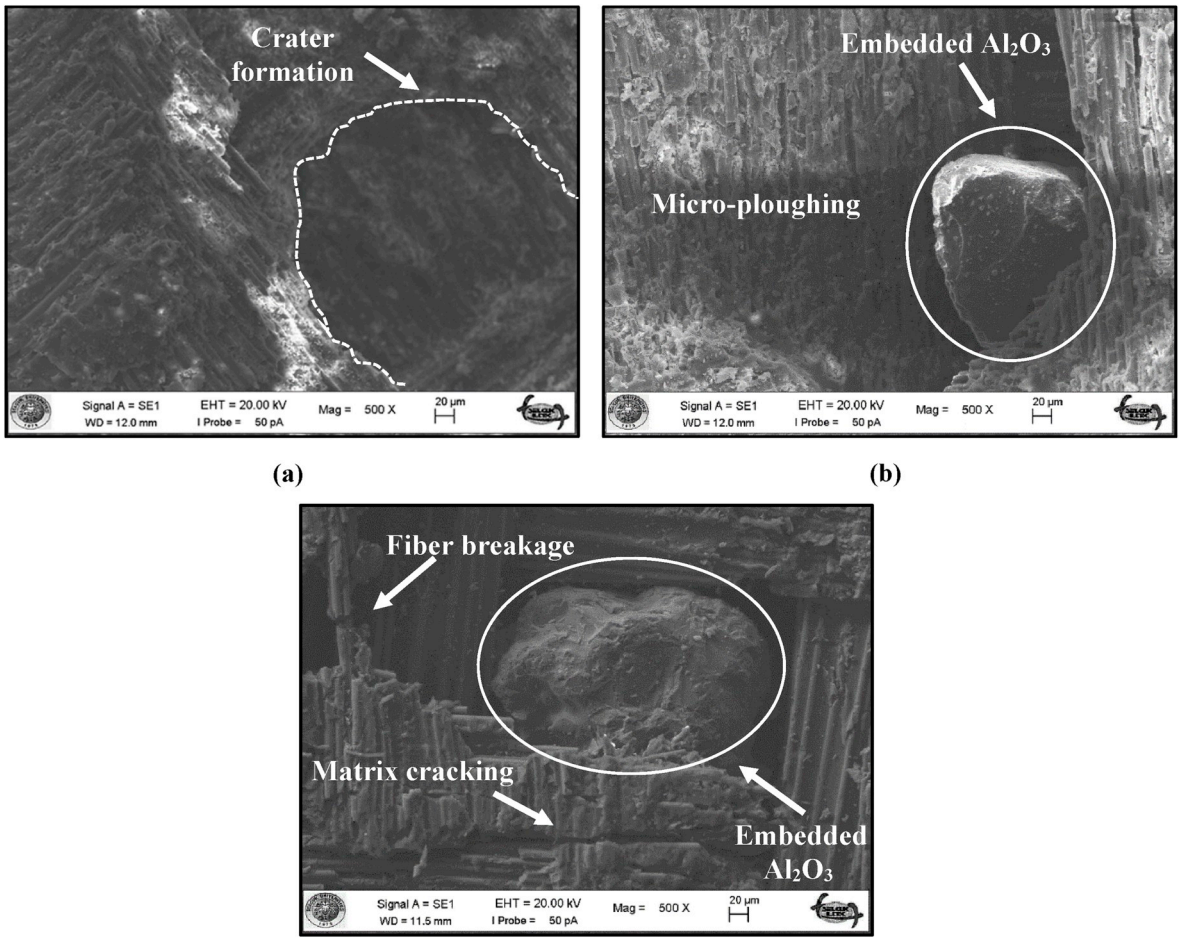


**Fig. 5.** SEM views of GF/epoxy test specimens (34 m/s impact velocity): a) 30°, b) 60° and c) 90°.

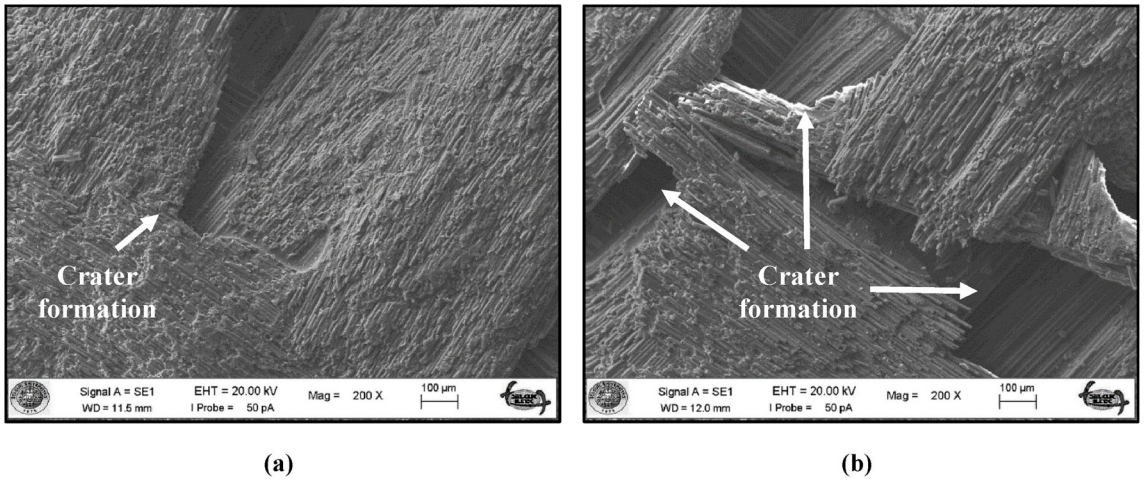


**Fig. 6.** SEM views of GF/epoxy test specimens (30° impingement angle): a) 23 m/s and b) 34 m/s.

energy of $Al_2O_3$ particles at 34 m/s when compared to that at 23 m/s.

### 3.2. Incubation period and steady-state erosion

By considering material loss as a function of impact time, we can clearly observe a developmental stage (the incubation period), which is a sign that the material is ductile. In this stage, the weight of the target material initially increases, and then, material loss begins, and erosion wear reaches a linearly increasing state. This period emerges because of the embedding of abrasive particles into the ductile target material. Steady-state erosion behaviour can be observed after these particles start to separate from the target material [25,26]. The literature shows that soft polymers such as polyethylene (PE), polypropylene (PP) and polybutene-1 (PB) exhibit an incubation period before transition to a

steady-state erosion rate [27]. Abrasive particles are more inclined to embed into the polymer surface at the starting stages of erosion wear, such as with a normal impingement angle (90°) [28]. When comparing polymers' glass-transition temperatures ($T_g$), polyetheretherketone (PEEK) and polyphenylene sulphide (PPS) have lower $T_g$ values than polyetherimide (PEI), polyethersulphone (PES) and polysulphone (PSU). Because of this property, the mass of PEEK and PPS polymers tends increase (incubation) at the starting stages of the erosion test. Hard, amorphous and solid polymers such as PEI, PES and PSU have a high $T_g$ and experience a transition to steady-state erosion without entering an incubation period during wear [29]. According to the conclusions of other studies in the literature, besides polymers, elastomers such as polyurethane also show a tendency to exhibit an incubation period [26,30]. They argued that a single impact is not enough to create the strain that would cause material separation from the surface in the case of the erosion mechanism. This erosion mechanism contains strain relaxation. However, several consecutive impacts are needed for this. This mechanism is explained by erosion resistance and an incubation period in more ductile materials such as elastomers and ultra-high-molecular-weight polyethylene (UHMWPE).

GF/epoxy (pure) test specimens exhibited a clearly noticeable incubation period before transition to steady-state erosion in erosive wear tests. To determine the transition from the incubation period to steady erosion, wear tests were conducted with 20 kg of abrasive particles. The tests were performed under unpressurised (moving with the weight of the particles) and pressurised (1, 2 and 3 bar) conditions in the mixing chamber with a 30° impingement angle. The mixing chamber is pressurised by the Pressure Regulator 1 located at the top of the mixing chamber. This pressurisation aims to prevent the retraction effect of the abrasive particles in the mixing chamber and arrange the test duration. When the mixing chamber reaches the desired pressure, the pressure is closed by the Pressure Regulator 1. By means of pressure regulator No. 2, erosion wear tests are performed by determining the impact velocity of the abrasive particles. Pressure Regulator 2 is directly connected to the nozzle and this controls the abrasive particle impact velocity. The abrasive particles were sent without pressurising the mixing chamber, and the test with 20 kg of abrasive particle lasted approximately 16 min. Afterwards, the pressure applied to the abrasive particles in the mixing chamber clearly influenced the transition period of the specimens from incubation to steady-state erosion, as shown in Fig. 7. Under the same conditions, specimens did not transition to steady-state erosion when the particles were not pressurised. Under pressures of 0, 1, 2 and 3 bar, the incubation period was completed in 16, 12, 8.5 and 3 min, respectively. Thereafter, material separation occurred on the surface of the specimen, and weight loss was observed. Because of the test duration was enough to see incubation period clearly and weight loss in steady-state erosion rate increased continuously, the applied pressure in the mixing chamber was taken as 1 bar at the experiments.

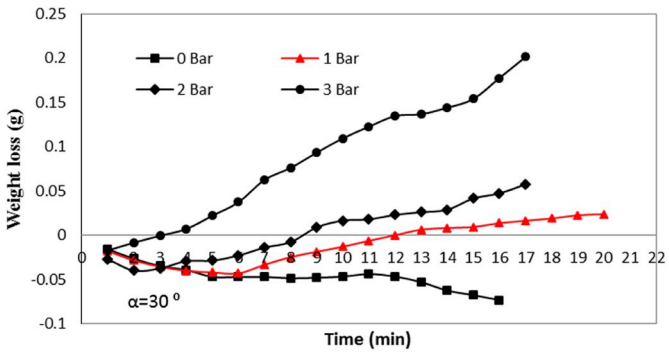


**Fig. 7.** Weight loss-time graph of GF/epoxy (pure) test specimens at different pressures in the mixing chamber and 34 m/s impact velocity and 30° impingement angle.

### 3.3. The effect of nanoclay addition

The effects of adding the nanoclay to the polymer matrix for tensile and flexural test are shown in Fig. 8. When the tensile test graph is examined, it can be seen that the strain under tension is higher in the nanocomposite material doped with 1% nanoclay compared to the GF/epoxy (pure) material. This shows a decrease in the 3% nanoclay-doped composite and GF/epoxy (pure) material, respectively. In tensile tests, it is also seen that the addition of nanoclay increases both the strength and ductility of the nanocomposite material (Fig. 8(a)). In the flexural test, the displacement is more in the 1% nanoclay-doped nanocomposite under axial load. Unlike tensile testing, displacement under axial load is higher in the pure material than in the 3% nanoclay-doped nanocomposite [Fig. 8(b)].

In summary, although the nanocomposite material exhibited ductile behaviour under normal stress, the specimen with 3% doping produced less displacement (ductility behaviour) than GF/epoxy (pure) under axial load. When the nanoclay particles are homogeneously dispersed in

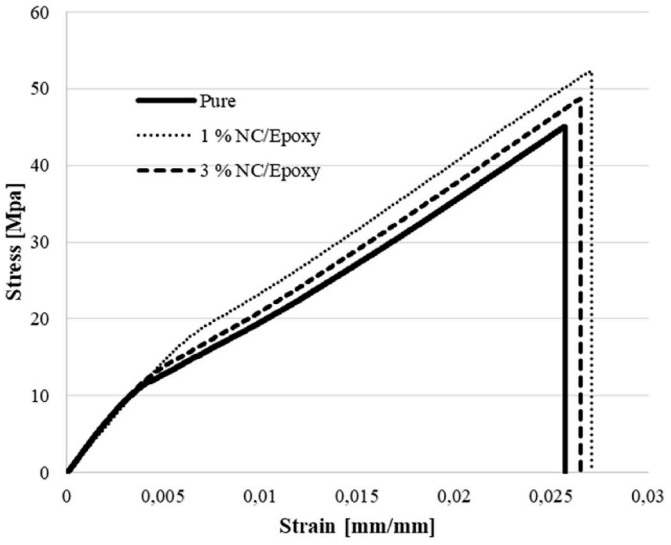


(a)

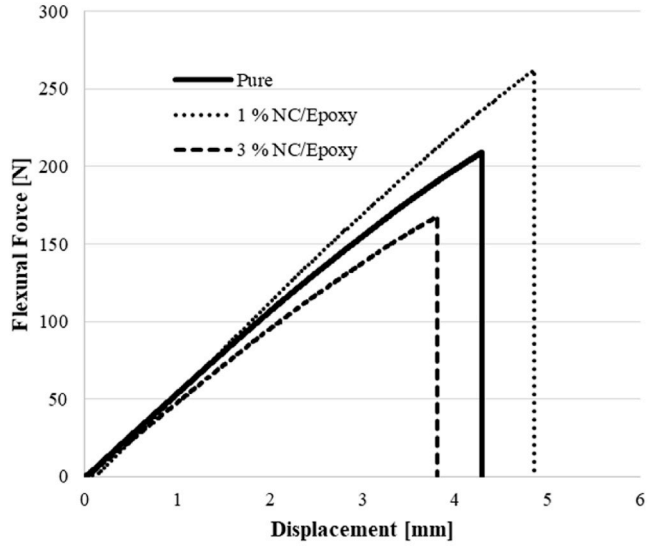


(b)

**Fig. 8.** Mechanical properties of Nanoclay/epoxy nanocomposites; a) Tensile test, b) Flexural test.

the polymer matrix, they form special bonding areas between particle/polymer/fibre within the material by means of unit surface areas. When damage and cracks spread through the special bonding areas with the effect of loading, there will be more energy needed for crack propagation, fibre breaking and matrix cracking. This means that a higher load is needed to break the material (strength increase). The plastic deformations occurring on the matrix under this load also determine the ductility behaviour of the material. In some cases, when a crack in the material encounters a nanoparticle, the crack propagates around the particle or in another direction instead of trying to break the nanoparticle. This (toughness) mechanism is expected to make a difference to erosion wear. In this case, the increased amount of plastic deformation on the material breaking surface causes the material to exhibit ductile behaviour in erosion wear.

Reinforcing the composite material with the addition of 1% and 3% nanoclay by weight affected the wear properties both positively and negatively. As can be seen in Fig. 9, the nanoclay additive changed the erosion rate of the composites. From erosion wear test results relying on effective erosion parameters such as impingement angle, impact velocity and abrasive mass, it was concluded that nanoclay addition to epoxy resins did not change the erosion wear mechanism of GF/epoxy composites.

The maximum erosion rate was observed at a 30° impingement angle in all test specimens [GF/epoxy (pure), 1% NC/epoxy and 3% NC/epoxy], and the specimens behaved like a ductile material. It can be observed that the erosion rates of 1% and 3% nanoclay-doped composites were higher compared to pure specimens. The erosion rate was approximately two times higher at a 30° impingement angle. This rate gradually decreased at a 60° impingement angle, whereas an increasing trend was observed at a 90° impingement angle.

According to the results, the addition of nanoclay had a negative effect on the wear properties of pure composites with 30° and 90° impingement angles, and the wear was relatively improved at a 60° impingement angle. In pure composites, an incubation period was observed with increasing angle of impingement. Furthermore, steady-state erosion occurred at all angles of impingement in 1% and 3% nanoclay-doped composites. The increased hardness of the composite material with the nanoclay reinforcement prevented the surface embedding of abrasive particles. Thus, the abrasive particles hitting the surface of specimens caused material separation at the surface of the composite, and erosion wear occurred. The drop in the hardness value can be explained by the addition of secondary particle phases with a lower hardness value compared to the matrix.

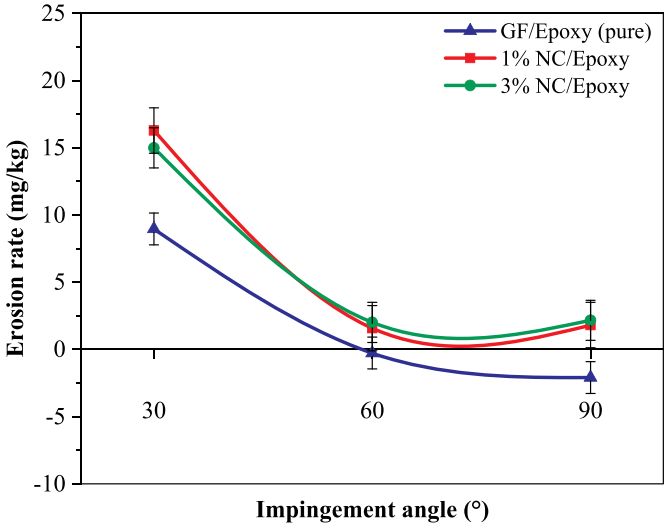


**Fig. 9.** The relationship between the impingement angle and the erosion rate of the test specimens at 34 m/s impact velocity.

The poor physical interaction (poor adhesion) between the polymer and the clay leads to poor mechanical and thermal properties [31]. In addition to the poor adhesion between the polymer matrix and the clay, a possible agglomeration at high weight loading of the clay, local stress concentration and consequently to the filler–filler interaction leads to a reduction in the mechanical properties of the nanocomposites [32].

Pure composites without the addition of a filler material exhibited the lowest wear rate, which is related to their high bonding strength. In brief, pure composite specimens are proportionally more resistant to wear when compared to nanoclay-doped specimens. It could be said that adding nanoclay to the matrix weakens the bonds. The addition of 1% nanoclay increased the tensile strength of composites, whereas a decrease was observed with the addition of 3% nanoclay. This is due to the non-homogeneous distribution of the particles within the structure as a result of the increase of the percentage of nanoclay. As the particle density increases, the particles start to exhibit a clustering tendency. Thus, bonds are weakened, and strain appears around the particles, which causes weakening in the mechanical properties of the composite.

Analysis of SEM images shows that the erosion resistance effect has a similar trend with different magnifications (Fig. 10). It was concluded that the matrix–epoxy interaction of pure test specimens, in comparison to those with added nanoclay, did not disrupt the bond structure. Consequently, it was found that erosion resistance was higher in pure specimens as compared to the other specimens. It was clearly observed in SEM images that erosion resistance in 1% and 3% nanoclay-doped specimens was weak, especially because of the weak bond effect at the matrix–fibre interface. Weak bonding strengths in 3% nanoclay-doped specimens facilitated the material separation by the abrasive particles, which increased the wear. In addition to the effect on bonding strength in 1% nanoclay-doped specimens, nanoclay addition caused structural adherence, which moderately reacted to the abrasive particles [Fig. 10 (b)]. Owing to the weak bond strength, abrasive particles in 3% nanoclay-doped composites increased erosion wear by causing the material to easily separate from the surface. Therefore, wear resistance was higher in pure specimens as compared to 3% nanoclay-doped specimens.

## 4. Conclusions

In this study, solid particle erosion tests were used to experimentally analyse the wear behaviour of nanoclay-doped glass fibre/epoxy nanocomposites. The following conclusions can be drawn:

- An incubation period was observed at both impact velocities (23 and 34 m/s), and particularly at 60° and 90° impingement angles, the weights of the test specimens increased depending on the acting abrasive particles.
- Whether nanoclay is added or not, all test specimens behaved like ductile materials, which showed a maximum erosion rate at a 30° impingement angle. In these test specimens, as the impingement angle increased, the erosion rate decreased.
- Although there was variability in error bars, generally the erosion rate of the tested specimens increased with an increase in the impact velocity.
- The mechanical properties of nano-modified composites were improved when nanoclay was added at 1% by weight. However, the mechanical properties decreased at 3% nanoclay by weight.
- The addition of nanoclay in different proportions negatively influenced the erosion wear characteristics of composites by causing an increase in erosion rates. From SEM images, the lowest erosion rate was exhibited by GF/epoxy (pure) because of its strong adhesive strength.
- Significant differences were observed in erosion wear properties between 1% and 3% nanoclay addition. Although the nanoclay effect was first negative at a 30° impingement angle, the erosion rate was increased to a certain extent with the increasing proportion of nanoclay particle, thus revealing the authenticity of this study.

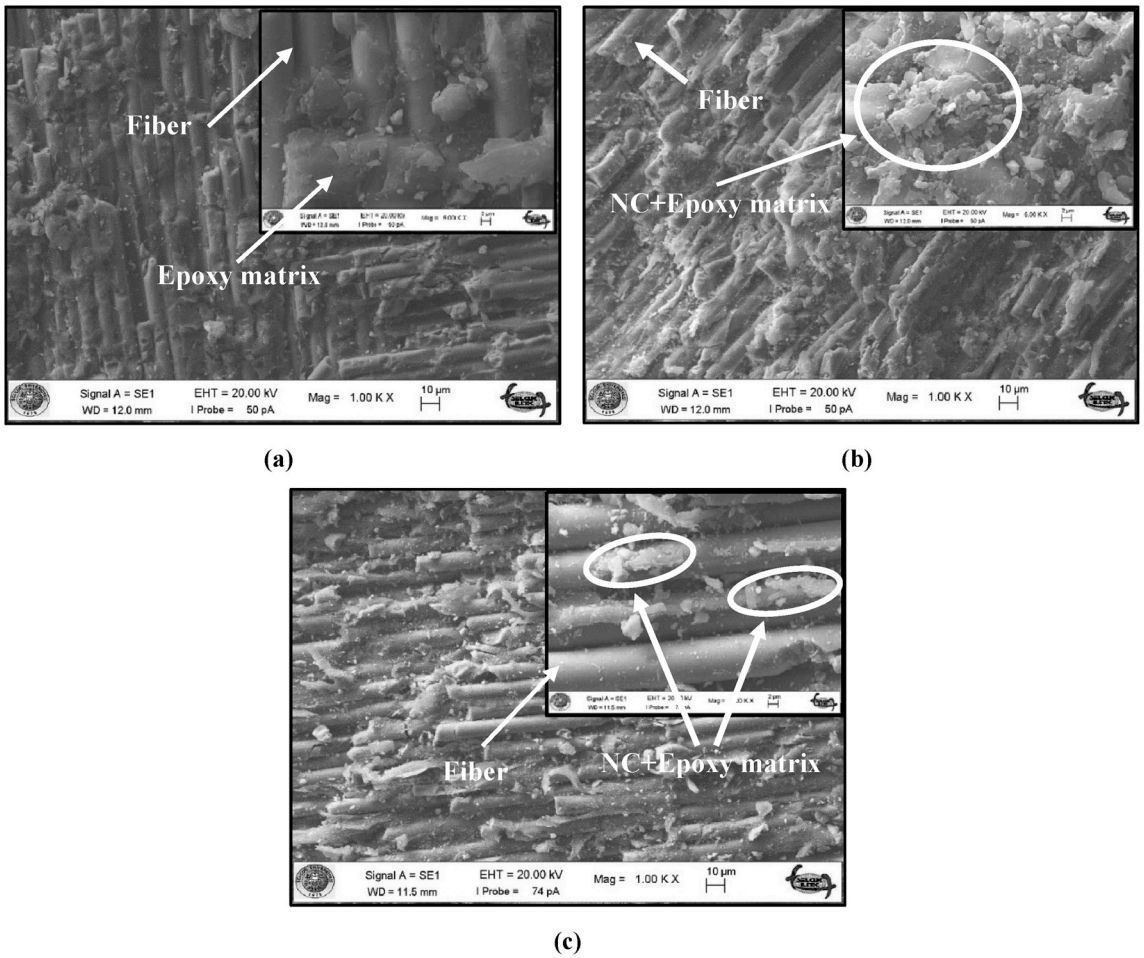


**Fig. 10.** SEM views of test specimens after wear at 34 m/s impact velocity and 30° impingement angle: (a) GF/epoxy (pure); (b) 1% NC/epoxy; (c) 3% NC/epoxy.

- ➢ The mechanical properties of composites can be enhanced by nano-sized reinforcements. However, even if the mechanical properties are enhanced, the tribological properties may not be enhanced in parallel. This study shows that the addition of nanoclay can cause negative effects on materials' tribological properties, such as decreasing erosion wear resistance.
- ➢ When the experimental study and the results obtained are examined extensively, the use of nanoclay additions in different proportions should be considered to avoid particle embedding on material surfaces in environments exposed to erosion wear in industrial applications.

## Declaration of competing interests

The authors declare that they have no known competing financial interests or personal relationships that could have appeared to influence the work reported in this paper.

## Appendix A. Supplementary data

Supplementary data to this article can be found online at https://doi.org/10.1016/j.wear.2019.203159.

## References

[1] T. Sinmazçelik, S. Fidan, V. Günay, Residual mechanical properties of carbon/polyphenylenesulphide composites after solid particle erosion, Mater. Des. 29 (2008) 1419–1426, https://doi.org/10.1016/j.matdes.2007.09.003.

[2] M. Bagci, H. Imrek, Solid particle erosion behaviour of glass fibre reinforced boric acid filled epoxy resin composites, Tribol. Int. 44 (2011) 1704–1710, https://doi.org/10.1016/j.triboint.2011.06.033.

[3] M. Bagci, Determination of solid particle erosion with Taguchi optimization approach of hybrid composite systems, Tribol. Int. 94 (2016) 336–345, https://doi.org/10.1016/j.triboint.2015.09.032.

[4] S.K. Mishra, S. Biswas, A. Satapathy, A study on processing, characterization and erosion wear behavior of silicon carbide particle filled ZA-27 metal matrix composites, Mater. Des. 55 (2014) 958–965, https://doi.org/10.1016/j.matdes.2013.10.069.

[5] N. Mohan, C.R. Mahesha, B.M. Rajaprakash, Erosive wear behaviour of WC filled glass epoxy composites, Procedia Eng. 68 (2013) 694–702, https://doi.org/10.1016/j.proeng.2013.12.241.

[6] S. Mohapatra, S. Mantry, S.K. Singh, A. Satapathy, Solid particle erosion behavior of glass-epoxy composites filled with TiC derived from ilmenite, Int. J. Plast. Technol. 18 (2014) 75–87, https://doi.org/10.1007/s12588-014-9066-z.

[7] J. Chen, J.A. Trevarthen, T. Deng, M.S.A. Bradley, S.S. Rahatekar, K.K.K. Koziol, Aligned carbon nanotube reinforced high performance polymer composites with low erosive wear, Compos. Appl. Sci. Manuf. 67 (2014) 86–95, https://doi.org/10.1016/j.compositesa.2014.08.009.

[8] A. Papadopoulos, G. Gkikas, A.S. Paipetis, N.M. Barkoula, Effect of CNTs addition on the erosive wear response of epoxy resin and carbon fibre composites, Compos. Appl. Sci. Manuf. 84 (2016) 299–307, https://doi.org/10.1016/j.compositesa.2016.02.012.

[9] X. Sun, Y. Wang, D.Y. Li, C. Wang, X. Li, Z. Zou, Solid particle erosion behavior of carbidic austempered ductile iron modified by nanoscale ceria particles, Mater. Des. 62 (2014) 367–374, https://doi.org/10.1016/j.matdes.2014.05.042, 1980-2015.

[10] F.H. Gojny, M.H.G. Wichmann, B. Fiedler, K. Schulte, Influence of different carbon nanotubes on the mechanical properties of epoxy matrix composites – a comparative study, Compos. Sci. Technol. 65 (2005) 2300–2313, https://doi.org/10.1016/j.compscitech.2005.04.021.

[11] B.J. Njuguna, K. Pielichowski, J.R. Alcock, Epoxy-based fibre reinforced nanocomposites, Adv. Eng. Mater. 9 (2007) 835–847, https://doi.org/10.1002/adem.200700118.

[12] N. Sapiai, A. Jumahat, N. Manap, M.A.I. Usoff, Effect of nanofillers dispersion on mechanical properties of clay/epoxy and silica/epoxy nanocomposites, J. Teknol. 76 (2015) 103–109, https://doi.org/10.11113/jt.v76.5687.
[13] A. Jumahat, A.A.A. Talib, A. Abdullah, Wear properties of nanoclay filled epoxy polymers and fiber reinforced hybrid composites, in: M. Jawaid, A.e.K. Qaiss, R. Bouhfid (Eds.), Nanoclay Reinforced Polymer Composites: Nanocomposites and Bionanocomposites, Springer Singapore, Singapore, 2016, pp. 247–260, https://doi.org/10.1007/978-981-10-1953-1_11.
[14] W.D.J. Callister, D.G. Rethwisch, Materials Science and Engineering, An Introduction, 2014.
[15] A. Jumahat, C. Soutis, N. Ahmad, W.M. Wan Mohamed, Fracture toughness of nanomodified-epoxy systems, Appl. Mech. Mater. 393 (2013) 206–211. 10.4028/www.scientific.net/AMM.393.206.
[16] A. Jumahat, C. Soutis, F.R. Jones, A. Hodzic, Compressive behaviour of nanoclay modified aerospace grade epoxy polymer, Plast., Rubber Compos. 41 (2012) 225–232, https://doi.org/10.1179/1743289811Y.0000000028.
[17] B. Sharma, S. Mahajan, R. Chhibber, R. Mehta, Glass fiber reinforced polymer-clay nanocomposites: processing, structure and hygrothermal effects on mechanical properties, Procedia Chem. 4 (2012) 39–46, https://doi.org/10.1016/j.proche.2012.06.006.
[18] A. Rafiq, N. Merah, R. Boukhili, M. Al-Qadhi, Impact resistance of hybrid glass fiber reinforced epoxy/nanoclay composite, Polym. Test. 57 (2017) 1–11, https://doi.org/10.1016/j.polymertesting.2016.11.005.
[19] R. Sridhar, H.N.N. Murthy, G. Angadi, N. Raghavendra, S. Firdosh, M. Krishna, Effect of nanoclay addition on the erosion wear of glass/vinylester composites using taguchi's orthogonal array technique, Procedia Mater. Sci. 5 (2014) 1174–1181, https://doi.org/10.1016/j.mspro.2014.07.414.
[20] I. Finnie, J. Wolak, Y. Kabil, J. Mater. Sci. 2 (1967) 682–700.
[21] R.H. Barkalow, J.A. Goebel, F.S. Pettit, Erosion corrosion of coatings and superalloys in high-velocity hot gases, Erosion: prevention and useful applications, ASTM STP 664 (1979) 163–192, https://doi.org/10.1520/STP35801S.
[22] A.J. Ninham, I.M. Hutchings, Proceedings of the 6th International Conference on Erosion by Liquid and Solid Impact, University of Cambridge, 1983, pp. 50–51.
[23] S.M. Walley, J.E. Field, P. Yennadhiou, Single solid particle impact erosion damage on polypropylene, Wear 100 (1984) 263–280, https://doi.org/10.1016/0043-1648(84)90016-4.
[24] S.M. Walley, J.E. Field, M. Greengrass, An impact and erosion study of polyetheretherketone, Wear 114 (1987) 59–72, https://doi.org/10.1016/0043-1648(87)90016-0.
[25] G.P. Tilly, Erosion caused by airborne particles, Wear 14 (1969) 63–79, https://doi.org/10.1016/0043-1648(70)90171-7.
[26] J.C. Arnold, I.M. Hutchings, The mechanisms of erosion of unfilled elastomers by solid particle impact, Wear 138 (1990) 33–46, https://doi.org/10.1016/0043-1648(90)90166-8.
[27] K. Friedrich, Erosive wear of polymer surfaces by steel ball blasting, J. Mater. Sci. 21 (1986) 3317–3332, https://doi.org/10.1007/bf00553375.
[28] H. Getu, J.K. Spelt, M. Papini, Conditions Leading to the Embedding of Angular and Spherical Particles during the Solid Particle Erosion of Polymers, " Wear, 2012, pp. 159–168, https://doi.org/10.1016/j.wear.2012.05.017.
[29] S. Arjula, A.P. Harsha, M.K. Ghosh, Solid-particle erosion behavior of high-performance thermoplastic polymers, J. Mater. Sci. 43 (2008) 1757–1768, https://doi.org/10.1007/s10853-007-2405-0.
[30] G.P. Tilly, W. Sage, The interaction of particle and material behaviour in erosion processes, Wear 16 (1970) 447–465, https://doi.org/10.1016/0043-1648(70)90171-7.
[31] M.Y. Abdelaal, M.A. Hussein, A.M. Alosaimi, et al., An overview on polysulphone/clay nanocomposites, Int. J. Biosens. Bioelectron. 3 (1) (2017) 201–205, https://doi.org/10.15406/ijbsbe.2017.03.00049.
[32] M. Somaiah Chowdary, M.S.R.N. Kumar, Effect of nanoclay on the mechanical properties of polyester and S-Glass fiber (Al), Int. J. Adv. Sci. Technol. 74 (2015) 35–42.